Microfluidics and Nanofluidics (2018) 22:142
https://doi.org/10.1007/s10404-018-2163-0

RESEARCH PAPER

Picking up and placing a liquid marble using dielectrophoresis

Chin Hong Ooi[1] · Jing Jin[1] · Anh V. Nguyen[2] · Geoffrey M. Evans[3] · Nam-Trung Nguyen[1]

Received: 18 July 2018 / Accepted: 8 November 2018 / Published online: 21 November 2018

Abstract
A liquid marble is a droplet coated with hydrophobic powder. The porous and hydrophobic coating prevents physical contact between the liquid and its surroundings without compromising gas exchange. As such, the liquid marble is an excellent platform for culturing cells. With the promising biomedical applications of the liquid marble, numerous studies have been conducted to improve its handling using magnetism, which limits the liquid marble coating to hydrophobised ferromagnetic materials. In this paper, we propose a novel, simple and cheap method of liquid marble manipulation such as pick and place based on the well-known dielectrophoresis force. Liquid marbles of various volumes were picked up using an electrode with a high voltage bias, moved to a different location and placed intact. This method provides reliable handling to a host of existing non-ferromagnetic liquid marbles without the need to engineer their coatings. Furthermore, this method enables the automation of the liquid marble handling process. This paper provides an empirical relationship to link the pickup force to the experimental parameters.

1 Introduction

A liquid marble can be manipulated using various means as reported in a number of recent review articles (Aussillous and Quere 2001, 2006; Bormashenko 2011, 2012, 2017; McHale and Newton 2011, 2015; Ooi and Nguyen 2015). Most of the manipulation methods used the electromagnetic (Bormashenko et al. 2008; Dorvee et al. 2004; Khaw et al. 2017, 2016; Lin et al. 2016; Long et al. 2009; Ooi et al. 2016b; Xue et al. 2010; Zhao et al. 2010, 2012; Zhu et al. 2011) or thermocapillary forces (Bormashenko et al. 2015; Kavokine et al. 2016; Ooi et al. 2015a; Paven et al. 2016). For instance, droplets and liquid marbles can move across electrode arrays owing to the electrowetting phenomenon (Newton et al. 2007). Magnetic liquid marbles can move across solid (Xue et al. 2010; Zhao et al. 2010, 2012) and liquid surfaces (Han et al. 2016; Khaw et al. 2017, 2016; Ooi et al. 2016b; Zhang et al. 2012) under the influence of a magnetic field. These marbles can even be picked up vertically, which enables three-dimensional (3D) digital microfluidics handling. Since a liquid marble has a porous coating and can float on liquid surfaces (Dupin et al. 2009; Fujii et al. 2011; Nakai et al. 2013; Ooi et al. 2016c, 2015b), it has become a useful platform for culturing cells (Arbatan et al. 2012; Oliveira et al. 2017; Sarvi et al. 2015; Tian et al. 2013; Vadivelu et al. 2015). Recently, the acoustic field had been used to levitate and even coalesce liquid marbles (Chen et al. 2017; Zang et al. 2015).

Despite the numerous manipulation methods, hardly any method offers 3D handling except magnetic liquid marbles. Consequently, many researchers still rely heavily on manual handling of liquid marbles, such as pick and place using a spatula. Manual handling incurs negligible equipment cost but it is time consuming, inconsistent and has a relatively high chance of breaking the liquid marble. As such, substantial efforts have been invested on studying the robustness of a liquid marble (Zang et al. 2013). Researchers dealing with liquid marbles are often forced

This article is part of the topical collection "2018 International Conference of Microfluidics, Nanofluidics and Lab-on-a-Chip, Beijing, China" guest edited by Guoqing Hu, Ting Si and Zhaomiao Liu

Electronic supplementary material The online version of this article (https://doi.org/10.1007/s10404-018-2163-0) contains supplementary material, which is available to authorized users.

✉ Chin Hong Ooi
chinhong.ooi@griffithuni.edu.au

[1] Queensland Micro-and Nanotechnology Centre, Griffith University, 170 Kessels Road, Nathan, QLD 4111, Australia

[2] School of Chemical Engineering, University of Queensland, St Lucia, QLD 4072, Australia

[3] Department of Chemical Engineering, University of Newcastle, Callaghan, NSW 2308, Australia

to remake broken marbles, which can be expensive if the liquid marbles contain valuable reagents or biological samples. Therefore, we designed a simple device which can pick and place liquid marbles reliably.

We selected the DEP force to manipulate the liquid marble as this method can be used for researchers who engineered liquid marble coatings for highly specific purposes (Bhosale et al. 2008; Mele et al. 2014; Miao et al. 2014; Ogawa et al. 2014; Ueno et al. 2014). Our method also caters to liquid marbles made from widely-available hydrophobic compounds such as polytetrafluoroethylene (PTFE), polyvinylidene fluoride (PVDF), lycopodium, graphite or polyethylene (PE). As such, researchers will be able to use the DEP force to pick and place their specialised liquid marbles without introducing hydrophobised magnetic particles, which would introduce unknown effects and might interfere with the intended function of the engineered marble coating.

When a liquid marble is placed in a strong and uniform electric field, the generated DEP force deforms the marble (Bormashenko et al. 2012a, b). Liu et al. (2017) showed that the marble coating can be destabilised using a strong DC electric field to achieve coalescence. This paper extends this concept by integrating DEP with the principles of electrostatic micrograpping (Biganzoli and Fantoni 2008; Fantoni and Biganzoli 2004; Hesselbach et al. 2001). The reported electrostatic micrograpper could pick up very small solid objects and has a self-centering capability when the electrode was printed in particular shapes on the glass slide. Inspired by prior research in this area, we modified the electrode setup to demonstrate our proof of concept.

We exploit the DEP force by modifying the setup used by Bormashenko et. al. (Bormashenko et al. 2012a). Instead of generating a uniform electric field, we used a non-uniform electric field to pick up a sessile liquid marble and attach it to the top electrode. We also shield the electrode with a piece of electric tape to prevent electric charge deposition on the marble which could generate strong repulsive forces. Moreover, the electric tape was coated with PTFE powder to ensure that the liquid marble does not wet the tape during picking. This coating also facilitates marble release when the electrode was de-energised.

To generate high voltage without using expensive and bulky power supplies, we used a DC–DC high voltage converter. This pocket-sized module can be powered by a battery and a voltage regulator. Nonetheless, we used a benchtop power supply to drive the high voltage converter in our experiments for monitoring purposes. Our setup is significantly more powerful than existing designs as we were able to lift larger and heavier objects. Using this setup, we were able to pick and place marbles up to 25 µL which weighs about 25 mg.

2 Theory

This section discusses the established theories with regards to DEP force and the numerical model based on it. The DEP force in its general form can be expressed as (Wang et al. 1997):

$$\vec{F}_{DEP} = \oint \vec{\vec{T}} \cdot \vec{n} dA, \tag{1}$$

where $\vec{\vec{T}}$ is the Maxwell stress tensor and $\vec{n}$ is the surface normal vector. The DEP force can be obtained via the surface integral of the dot product of $\vec{\vec{T}}$ and $\vec{n}$. The stress tensor $\vec{\vec{T}}$ can be written as:

$$\vec{\vec{T}} = \frac{1}{2}\left[\vec{D}\vec{E} + \vec{E}\vec{D} - \left(\vec{E}\cdot\vec{D}\right)\vec{\vec{I}}\right], \tag{2}$$

where $\vec{E}$ is the electric field, $\vec{D}$ is the electric displacement field, $\vec{I}$. is the unit tensor, and vector products without notations are dyadic products of each other. Note that the magnetic field component has been omitted as we consider stationary fields only. Assuming a linear relationship between $\vec{E}$. and $\vec{D}$., Eq. (2) can be rewritten as (Wang et al. 1997):

$$\vec{\vec{T}} = \mathrm{Re}\left(\varepsilon_c\right)\left[\vec{E}\vec{E} - \frac{1}{2}\left(\vec{E}\cdot\vec{E}\right)\vec{\vec{I}}\right], \tag{3}$$

where $\mathrm{Re}\left(\varepsilon_c\right)$ is the real part of the complex peittivity of the media. In the case of a DC electric field, is equal to the permittivity of the media ε. Due to the complexity of the governing equations, we modelled the DEP force derived from a two-dimensional axisymmetric model.

First, the electric field is generated for the e.re model domain by setting Dirichlet boundary conditions (i.e. applied voltage) for the electrode and ground edges. Permittivity values were then applied for all objects within the model. Using MATLAB® PDE function, the electric field at every point of .he domain was generated as:

$$\vec{E} = -\nabla U, \tag{4}$$

where U is the scalar potential field. With. nown electric field, the stress tensor can be calculated for the entire domain as well. Next, by assuming the cross section of the liquid marble to be a circle with the coordinate origin at its centre, the surface normal vector at position (x,y) is simply

$$\vec{n}(x,y) = \frac{1}{|\vec{r}|}(x\hat{i} + y\hat{j}), \tag{5}$$

where r is the radius of the circle, $\hat{i}$ is the unit vector in the horizontal x direction and is the unit vector in the vertical y direction.

By combining Eqs. (3) and (5) into (1), the DEP force along a half-circle arc can be calculated. The vertical component of these forces were subsequently revolved around

the axis of symmetry and integrated to yield the effective DEP force in the vertical direction.

3 Materials and methods

3.1 Liquid marble preparation

Liquid marbles were prepared in a conventional "rolling droplet in a powder bed" method. A droplet of DI water (resistivity $\approx 1.8 \times 10^5$ Ω•m) was dispensed onto a PTFE pder (Sigma–Aldrich® nominal diameter of 1 µm) bed using a micropipette (Thermo Scientific Finnpipette 4500 0.5–10 µL) to ensure high accuracy. The droplet was then rolled around in the powder bed to form a liquid marble. Next, the liquid marble was carefully scooped out using a stainless steel teaspoon and placed on a microscope glass slide coated with PTFE powder.

3.2 Experimental setup

The liquid marble was placed on a microscope glass slide coated with PTFE powder. A thin, cylindrical, stainless steel electrode (diameter of 0.8 mm) was held a few millimetres above the liquid marble. The electrode was held vertically in place by an acrylic housing attached to a three-axis linear stage, Fig. 1. The bottom end of the electrode was shielded from the liquid marble with a piece of PVC electrical tape whereas the top end was connected to a high voltage bias. This bias was provided using a high voltage DC–DC converter (Eastern Voltage Research HVPS 2) driven by a benchtop power supply. The electrode was energised first, and then slowly lowered towards the sessile liquid marble. Once the liquid marble was picked up, the electrode was moved horizontally to a different location and then de-energised to release the liquid marble. This process was repeated three times for error measurements. A high speed camera (Photron Fastcam SA3) was used to record the side view of the entire pick and place process. Video recordings were conducted at 125 frames per second with a resolution of 512×1024 pixels. All of the experiments were conducted in a controlled environment of 22.5 ± 1 °C and a relative humidity of $55 \pm 5\%$. The recorded videos were analysed using ImageJ (National Institutes of Health, USA).

As PTFE is one of the most electronegative materials on the triboelectric series, electrostatic generation becomes an issue. PTFE powder can be charged when in contact with the experimental setup equipment such as the PVC electrical tape, the microscope glass slide, the acrylic electrode holder as well as nitrile gloves. Therefore, an ioniser fan was placed in the proximity of the experimental setup to remove electrostatic build up.

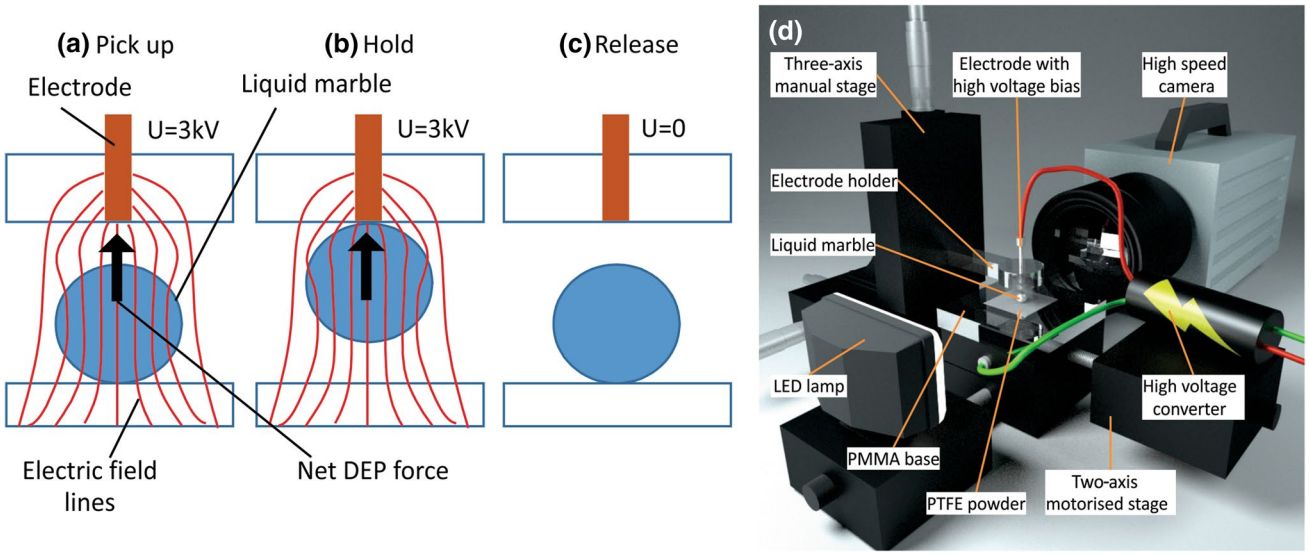

Fig. 1 Schematic of the operation principle and the experimental setup. **a** Initially, the electrode is biased to a high voltage. The non-uniform electric field generates a net upward DEP force which picks up the liquid marble. **b** As long as the electrode voltage is maintained, the liquid marble remains attached to the electrode. **c** When the electrode is de-energised, the liquid marble is released due to gravity and falls back onto the solid surface. **d** Experimental setup. Initially, the motorised stage was used to fix the liquid marble position with respect to the camera. Then, the electrode was moved using the manual stage to pick and place the liquid marble. The PMMA electrode holder and base plate ensured that the electrode did not arc towards any grounded component. The entire setup was mounted on a levelled optical breadboard which is not shown. The electrical tape at the bottom of the holder is not shown as well

4 Results and discussion

The output voltage of the converter was maintained at 2.9 kV for marble volumes ranging from 2 to 15 µL. This output was inadequate for larger marbles as they could not be picked up even with the electrode touching the top of the marble. Therefore, the output voltage was increased for experiments with 20 and 25 µL marbles. The minimum voltages required to pick up marbles of different volumes are listed in Table 1. Marbles ranging from 2 to 25 µL were successfully picked up and released intact. A lower output voltage is preferable to reduce ionisation and hence increase pick up consistency. Nonetheless, larger marbles are heavier and require higher voltages. As a result, experiments with larger marbles tend to yield larger errors.

Figure 2 shows the field distributions obtained from our numerical model with parameters obtained from the experimental setup as well as Table 1. The liquid marble is represented as a circular object with a thin PTFE coating sitting on a glass slide. The model includes critical components such as the electric terminals, the liquid marble and the insulating layers. The ground terminal is located at the bottom of the glass slide. All the components were drawn to scale and standard relative electrical permittivity values were used. The relative permittivity for air, water, glass, PTFE and PMMA are 1, 80, 10, 2.1, and 6, respectively. Details of the boundary conditions of the simulation are provided in the supplementary material Sect. 2. Deformation of the marble is not taken into account as it is coupled with the electric field distribution. The complexity involved in such a system is beyond the scope of this paper.

Figure 3 shows marbles of different volumes being picked up, moved horizontally and released. Sample videos are provided as electronic supplementary materials. Initially, the electrode was quite far from the sessile liquid marble. As the electrode was lowered, the marble was observed to deform and elongate in the direction of the increasing electric field, adopting the shape of a prolate spheroid. This phenomenon has been reported and elucidated by Bormashenko et al. (Bormashenko et al. 2012a). This effect is also shown in Fig. 2b where DEP forces at the top and bottom regions of the marble try to pull the marble apart, causing it to elongate. Figure 2b also shows that the electric field strength is highest in the small region between the top of the marble and the bottom of the electrode. The region within the marble and electrode has negligible electric field by comparison. Consequently, the electric field strength can be increased by

Table 1 The minimum output voltage required to pick up a sessile liquid marble

Marble volume (µL)	Output voltage (kV)
2	2.9
5	2.9
10	2.9
15	2.9
20	3.2
25	3.4

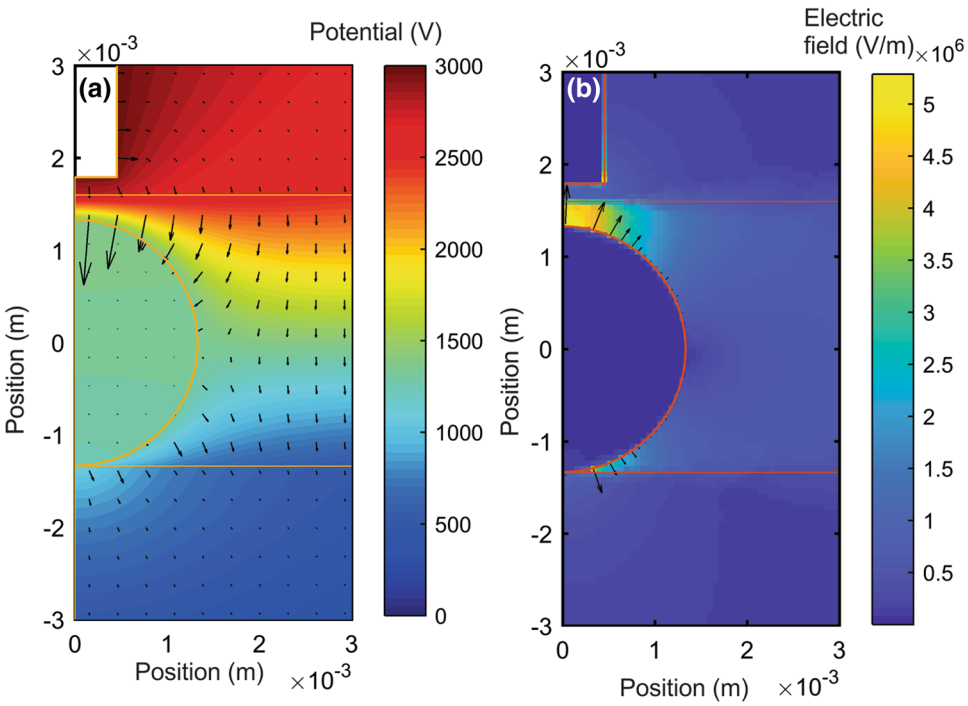

Fig. 2 An example of the numerical model of the potential and electric field in the vicinity of a 10 µL liquid marble with an electrode biased to 3 kV. **a** The surface colour map represents the potential field in V whereas the quiver plot represents the electric field. **b** The surface colour map represents the electric field strength in V/m whereas the quiver plot represents the DEP force acting on the surface of the liquid marble. All horizontal and vertical axes are in m

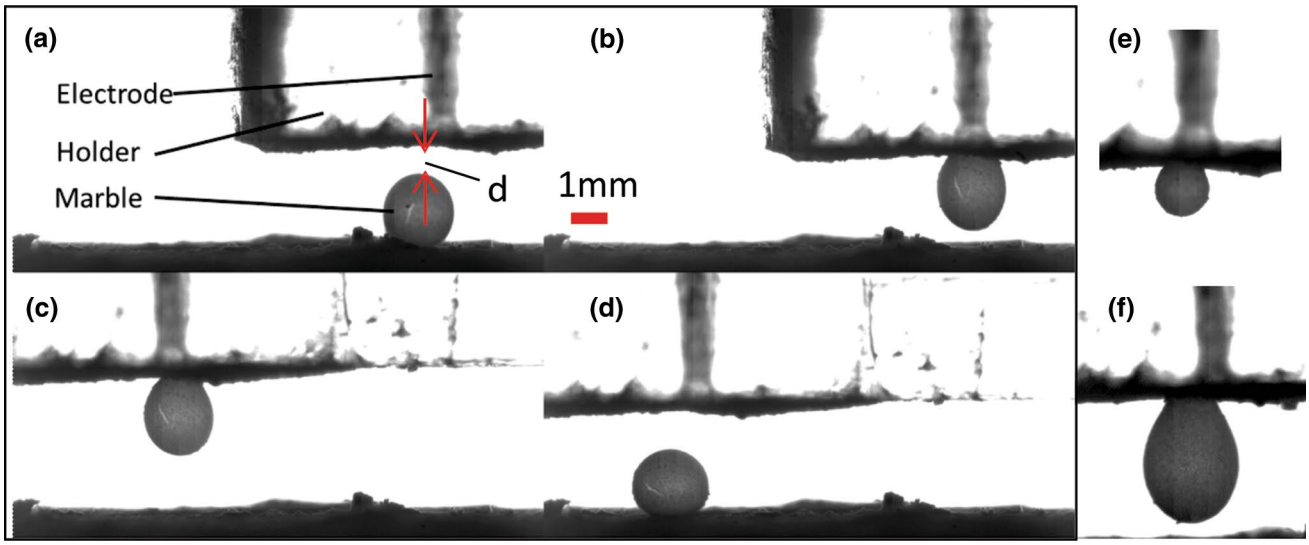

Fig. 3 Snapshots of a pick and place process of a 10 µL marble. **a** The electrode was brought closer to the marble, *d* refers to the distance between the top of the marble and the bottom of the electrode at the moment of pickup. **b** The marble was picked up by the electrode. **c** The electrode was moved to the left with the marble still attached. **d** The electrode was de-energised and the marble was released. **e** A small 2 µL marble retains its almost spherical shape when picked up. **f** A large 25 µL marble adopts a pendant shape when picked up

lowering the electrode towards the marble, even at a constant applied voltage.

Since the DEP forces were gradually increased by lowering the electrode onto the marble, we introduce the working distance as a convenient method to identify the marble pickup threshold. The working distance *d* is the distance measured between the top of the marble to the bottom of the electrode, Fig. 3a. Figure 4a shows the working distance for different marble volumes at the instance the marble was picked up. As the marble volume increases, a smaller working distance is required to generate a larger electric field and consequently larger DEP force to pick up the marble, as expected. A fitting curve was included to indicate the boundary between the pickup and non-pickup conditions. The relatively large error bars in Fig. 4a is attributed to the inconsistencies in the working distances for the repeated experiments. We hypothesise that these inconsistencies were due to the adhesion forces between the marble coating and the glass slide. As the glass slide used was coated with the same powder as the marble, some particles from the glass slide could be jammed into the marble coating, thus resisting the pickup force.

Figure 4b shows the comparison between the calculated DEP forces using the averaged working distance and the marble weights. Since the marble is picked up when the electrode is placed at the working distance, the generated DEP force should be equal or larger than the marble weight. However, our numerical model suggests otherwise. Although there is a similar increasing trend in the DEP force, the absolute value differs up to a factor of two. The numerical model consistently underestimates the effective DEP force. First, this is most likely due to the assumption of a rigid spherical marble. For small marbles, the surface tension force dominates over gravity and DEP forces so the marble remains relatively spherical. As the marble volume increases, the magnitude of the competing gravity and DEP forces dominate over surface tension force. Consequently, the marble elongates and its top apex reaches further into the high electric field strength region. With a larger portion of the marble in this high strength region, it is expected that the DEP force would be increased as well. This explains the divergence of the DEP force from the marble weight at larger marble volumes. To test this effect, we ran a numerical simulation to compare the DEP forces produced by elongated marble geometries. We approximated the marble shape as a prolate spheroid instead of a sphere. For this example, we used a 10-µl marble with a spherical radius of 1.3 mm. The deformed marble had a major axis of 1.35 mm and a minor axis of 1.2 mm. The unit vector defined in Eq. (5) was changed to $\vec{n}(x,y) = \left(0.92x\hat{i} + 1.04y\hat{j}\right)/\left|\vec{r}(x,y)\right|$ to cater for the ellipsoid. In this case, the calculated DEP force yielded 1.3 times the DEP force obtained from that of a spherical geometry. The simulation result is provided in the supplementary material Sect. 3. Second, the electric field distribution is quite sensitive to the electrode geometry. $F_{\mathrm{DEP}(y)} = k\varepsilon {U_0}^2$ The electrode in use could have some surface defects and slight positioning error which could cause deviation from the simulated condition. Third, the model assumes a uniform coating of PTFE powder on the marble surface for practical reasons. In practice, the coating is porous and filled with air pockets (Ooi et al. 2016a) which could affect the effective permittivity and consequently the

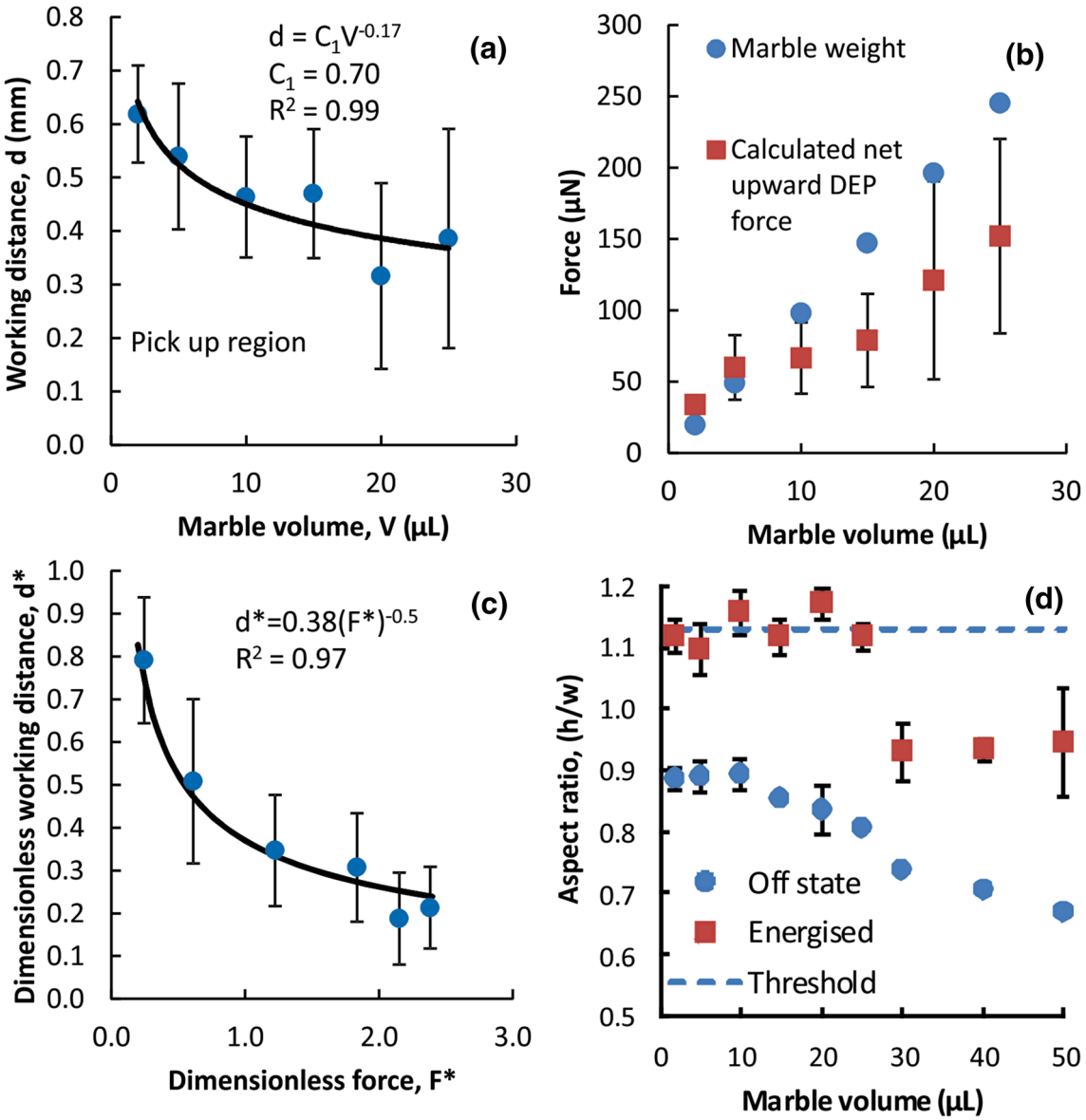

Fig. 4 Results obtained from the marble pick and place experiments. **a** Measured working distance versus marble volume. A fitting curve splits the graph into the pickup region at the bottom left and the non-pickup region at the top right, based on our experimental setup and parameters. **b** Marble weights and net upward DEP forces calculated using our numerical model. **c** Normalised working distance versus dimensionless force. A fitting line and its corresponding fitting parameters are shown as well. **d** Aspect ratio of various marble volumes at different electrode states. For marbles smaller than 25 µL, the aspect ratio is measured at the instance of lift off from the surface. As for larger marbles that could not be picked up, the aspect ratio is the maximum aspect ratio achievable with our current setup. The dashed line indicates the pickup threshold at 1.13

electric field distribution near the marble surface. To test this effect, we ran additional simulations by setting the relative permittivity of the coating to one, which implied that the coating consisted purely of air. This produced a slightly higher (~5%) calculated DEP force, as shown in supplementary material Sect. 3.

Despite the DEP force acting only on the surface of the liquid marble, it is convenient to treat the sum of the DEP force as a body force. For our case, the vertical component of the DEP force is summed up to yield the net upward DEP force, $F_{\mathrm{DEP}(y)}$. In this section, we attempt to form a relationship between the net upward DEP force and our experimental parameters.

From Eqs. (1), (3) and (4) it is clear tha. F_{DEP} scales with the Maxwell stress tensor T, such that:

$$\vec{F}_{\mathrm{DEP}} \propto \vec{\vec{T}} \propto \varepsilon \vec{E}^2 \propto \varepsilon \vec{U}_0^2, \tag{6}$$

where U_0 is the voltage of the electrode. As aforementioned the net upward DEP force $F_{DEP(y)}$ is a function of the working distance and the shape of the marble, Eq. (6) is thus modified to yield:

$$F_{DEP(y)} = k\varepsilon U_0^2, \tag{7}$$

where k is an unknown function of d^*, the dimensionless working distance in which $d^* = d/r$, and r is the radius of the non-deformed spherical marble:

$$r = \left(\frac{3V}{4\pi}\right)^{1/3}, \tag{8}$$

where V is the volume of the liquid marble. The dimensionless working distance is used to preserve dimensional consistency as well as to take into account the effect of both the working distance and the shape of the marble on the net upward DEP force. When the marble is picked up, we assume that the net upward DEP force is equal to the marble weight $V\rho g = F_{DEP(y)}$. Therefore, Eq. (7) can be rearranged to yield:

$$k = \frac{V\rho g}{\varepsilon {U_0}^2} = F^*, \tag{9}$$

where g is the gravitational acceleration, ρ is the effective density of the liquid marble and F^* is a dimensionless force which represents the ratio of gravity to capacitive force. Next, the fitting curve of d and V from Fig. 4a yields:

$$d = C_1 V^{-1/6}, \tag{10}$$

where C_1 is a constant which combines all the independent variables of gravity and the DEP force as well as the correction factor, which is not helpful. Thus, Eq. (10) is rewritten in its dimensionless form as:

$$\frac{d}{r} = \frac{C_1}{r\left(\frac{4}{3}\pi r^3\right)^{1/6}}, \tag{11}$$

$$\frac{1}{d*} = \frac{r^{3/2}\left(\frac{4}{3}\pi\right)^{1/6}}{C_1},$$

$$\frac{1}{d*} = \frac{V}{C_1^2\left(\frac{4}{3}\pi\right)^{2/3}} = C_2 V.$$

In this form, we can now compare Eq. (11) with (9) and separate the correction factor α from the independent variables.

$$\text{Let } C_2 = \frac{\rho g}{\alpha\varepsilon {U_0}^2} \text{ and } k = \frac{1}{(d^*)^2}, \qquad \frac{\alpha}{(d^*)^2} = \frac{V\rho g}{\varepsilon {U_0}^2} = F^*. \tag{12}$$

By plotting d^* against F^* in Fig. 4c and fitting a curve using Eq. (12), the correction factor α was found to be 2.63. Finally, the expression for $F_{DEP(y)}$ as a function of experimental parameters is:

$$F_{DEP(y)} = \frac{\alpha\varepsilon {U_0}^2}{(d*)^2} = \alpha\varepsilon\left(\frac{U_0 r}{d}\right)^2. \tag{13}$$

Equation (13) works well for the range of marble volumes and applied voltages used in this experiment. Also note that the liquid within the marble should have a relative permittivity much higher than that of the marble coating as well as its surrounding medium.

Analysis of the pickup threshold using the energy approach yields interesting results as well. For energy to be conserved, the electric energy received by the sessile marble must be converted to surface energy and gravitational potential energy. Here, we neglect other minor forms of energy output such as heat. The surface energy of the marble can be indirectly quantified by measuring the magnitude of deformation. In this case, we define the deformation of the marble as its aspect ratio, which is the vertical height divided by its horizontal width, h/w. For smaller marbles, we expect the ratio to be close to unity since surface tension dominates gravity forces. As the marble volume increases, the marble tends to flatten out which decreases the aspect ratio, Fig. 4d.

When an electric field is applied, the marble surface and gravitational potential energies increase and lead to a higher aspect ratio. Interestingly, all the marbles share very similar aspect ratios at the point of pickup, which is 1.13 ± 0.03 as shown in Fig. 4d. Larger marbles (> 25 µL) could only produce a maximum aspect ratio slightly below one, which resulted in no pickup. Since the aspect ratio is independent of marble volume, it seems that the surface energy of a sessile marble has a saturation point that needs to be met for pickup to occur. Once the saturation point is achieved, the electrical input energy is then converted to kinetic and gravitational potential energies, lifting the marble rapidly towards the electrode.

A more optimised experimental setup could be used to pick up larger marbles, but the threshold aspect ratio might still be the same. Nevertheless, if very large marbles were used, such an aspect ratio might just be too high and caused the marble to split instead of being picked up. Future investigation using a more optimised setup will be required to determine its existence.

Occasionally, the marble attaches itself to the periphery of the electrode. This is most likely due to the cylindrical geometry of the electrode where the circular edge generates large electric fields. This issue can be addressed by filleting the edges, thus eliminating undesirable concentration of charges. Attempts to pick up 30 µL marbles were unsuccessful, despite an output voltage of over 6 kV and a normalised

working distance of approximately zero. Strong electric fields ($> 5 \times 10^6$ V/m) would be generated, which ionises the surrounding air and deposits charges on the surface of the liquid marble, causing it to wobble or repel. The destabilisation of the liquid marble indicates that further increasing the output voltage would no longer be useful. Instead, further optimisation of the electrode design and experimental setup could improve on this aspect. For future works, the electrode can be driven with a high voltage AC instead. By tuning the AC frequency, the liquid marble can be attracted or repelled with ease. Additionally, the applied voltage could be lowered as the permittivity component in Eq. (3) could be increased by fine tuning the AC frequency. In this experiment, we chose DC over AC for its significantly lower cost and smaller footprint.

5 Conclusion

This paper presents a working proof of concept to consistently picking up and releasing a sessile liquid marble. The experimental setup proposed could relocate marbles ranging from 2 to 25 μL. The marble was picked up using the DC DEP force which was generated using a small and low-cost high voltage converter with an output of around 3 kV. A numerical model was presented to illustrate the electric field and generated a DEP force. An empirical relationship was formulated to link the net upward DEP force to critical experimental parameters such as the marble volume, output voltage and working distance, thus providing a convenient method for parametric optimisation. The net upward DEP force was found to be proportional to the capacitive force and the inverse square of the normalised working distance. Finally, the experimental setup was analysed for future improvements. In spite of the limitations of this pick and place technique, it is well-suited to manipulate a variety of liquid marbles. This technique also enables the automation of the liquid marble handling.

Acknowledgements We acknowledge the Australian Research Council for the discovery Grant DP170100277.

References

Arbatan T, Al-Abboodi A, Sarvi F, Chan PP, Shen W (2012) Tumor inside a pearl drop. Adv Healthc Mater 1:467–469

Aussillous P, Quere D (2001) Liquid marbles Nature 411:924–927

Aussillous P, Quere D (2006) Properties of liquid marbles. Proc. R Soc A 462:973–999

Bhosale PS, Panchagnula MV, Stretz HA (2008) Mechanically robust nanoparticle stabilized transparent liquid marbles. Appl Phys Lett 93:034109

Biganzoli F, Fantoni G (2008) A self-centering electrostatic micrograpper. J Manufacturing Syst 27:136–144

Bormashenko E (2011) Liquid marbles: properties and applications. Curr Opin Colloid Interface Sci 16:266–271

Bormashenko E (2012) New insights into liquid marbles. Soft Matter 8:11018–11021

Bormashenko E (2017) Liquid marbles, elastic nonstick droplets: from minireactors to Self-propulsion Langmuir 33:663–669

Bormashenko E, Pogreb R, Bormashenko Y, Musin A, Stein T (2008) New investigations on ferrofluidics: ferrofluidic marbles and magnetic-field-driven drops on. superhydrophobic surfaces Langmuir 24:12119–12122

Bormashenko E, Pogreb R, Balter R, Gendelman O, Aurbach D (2012a) Composite non-stick droplets and their actuation with electric field. Appl Phys Lett 100:151601

Bormashenko E, Pogreb R, Stein T, Whyman G, Schiffer M, Aurbach D (2012b) Electrically deformable liquid marbles. J Adhes Sci Technol 25:1371–1377

Bormashenko E, Bormashenko Y, Grynyov R, Aharoni H, Whyman G, Binks BP (2015) Self-propulsion of liquid marbles: leidenfrost-like levitation driven by Marangoni flow. J Phys Chem C 119:9910–9915

Chen Z et al (2017) Liquid marble coalescence and triggered microreaction driven by acoustic levitation Langmuir 33:6232–6239

Dorvee JR, Derfus AM, Bhatia SN, Sailor MJ (2004) Manipulation of liquid droplets using amphiphilic, magnetic one-dimensional photonic crystal chaperones. Nat Mater 3:896–899

Dupin D, Armes SP, Fujii S (2009) Stimulus-responsive liquid marbles. J Am Chem Soc 131:5386–5387

Fantoni G, Biganzoli F (2004) Design of a novel electrostatic gripper J Manuf Sci Prod 6:163-80

Fujii S, Suzaki M, Armes SP, Dupin D, Hamasaki S, Aono K, Nakamura Y (2011) Liquid marbles prepared from pH-responsive sterically stabilized Latex Particles Langmuir 27:8067–8074

Han X, Lee HK, Lim WC, Lee YH, Phan-Quang GC, Phang IY, Ling XY (2016) Spinning liquid marble and its dual applications as microcentrifuge and miniature localized viscometer ACS. Appl Mater Interfaces 8:23941–23946

Hesselbach J, Buttgenbach S, Wrege J, Butefisch S, Graf C (2001) Centering electrostatic microgripper and magazines for microassembly tasks. Microrobitics and microassembly III, vol 4568, SPIE, Boston, MA, USA, pp 270–277

Kavokine N, Anyfantakis M, Morel M, Rudiuk S, Bickel T, Baigl D (2016) Light-driven transport of a liquid marble with and against surface flows. Angew Chem Int Edit 55:11183–11187

Khaw MK, Ooi CH, Mohd-Yasin F, Vadivelu R, John JS, Nguyen N-T (2016) Digital microfluidics with a magnetically actuated floating liquid marble Lab. on a Chip 16:2211–2218

Khaw MK, Ooi CH, Mohd-Yasin F, Nguyen AV, Evans GM, Nguyen N-T (2017) Dynamic behaviour of a magnetically actuated floating liquid marble. Microfluid Nanofluid 21:110

Lin X, Ma W, Wu H, Cao S, Huang L, Chen L, Takahara A (2016) Superhydrophobic magnetic poly(DOPAm-co-PFOEA)/Fe3O4/cellulose microspheres for stable liquid marbles. Chem Commun 52:1895–1898

Liu Z, Fu X, Binks BP, Shum HC (2017) Coalescence of electrically charged liquid marbles. Soft Matter 13:119–124

Long Z, Shetty AM, Solomon MJ, Larson RG (2009) Fundamentals of magnet-actuated droplet manipulation on an open hydrophobic surface Lab. on a Chip 9:1567–1575

McHale G, Newton MI (2011) Liquid marbles: principles and applications Soft Matter 7:5473–5481

McHale G, Newton MI (2015) Liquid marbles: topical context within soft matter and recent progress. Soft Matter 11:2530–2546

Mele E et al (2014) Biomimetic approach for liquid encapsulation with. nanofibrillar cloaks Langmuir 30:2896–2902

Miao YE, Lee HK, Chew WS, Phang IY, Liu T, Ling XY (2014) Catalytic liquid marbles: Ag nanowire-based miniature reactors for

highly efficient degradation of methylene blue. Chem Commun (Camb) 50:5923–5926
Nakai K, Fujii S, Nakamura Y, Yusa S-i (2013) Ultraviolet-light-responsive Liquid. Marbles Chem Lett 42:586–588
Newton MI, Herbertson DL, Elliott SJ, Shirtcliffe NJ, McHale G (2007) Electrowetting of liquid marbles. J Phys D 40:20–24
Ogawa S, Watanabe H, Wang L, Jinnai H, McCarthy TJ, Takahara A (2014) Liquid marbles supported by monodisperse poly(methylsilsesquioxane Particles Langmuir 30:9071–9075
Oliveira NM, Reis RL, Mano JF (2017) The potential of liquid marbles for Biomedical applications: a critical review Adv Healthc Mater 6:1700192-(n/a)
Ooi CH, Nguyen N-T (2015) Manipulation of liquid marbles Microfluid Nanofluid 19:483–495
Ooi CH, Nguyen AV, Evans GM, Gendelman O, Bormashenko E, Nguyen N-T (2015a) A floating self-propelling liquid marble containing aqueous ethanol solutions. RSC Adv 5:101006–101012
Ooi CH, Vadivelu RK, St John J, Dao DV, Nguyen N-T (2015b) Deformation of a floating liquid marble. Soft Matter 11:4576–4583
Ooi CH, Bormashenko E, Nguyen AV, Evans GM, Dao DV, Nguyen N-T (2016a) Evaporation of ethanol–water binary mixture sessile liquid marbles Langmuir 32:6097–6104
Ooi CH, Nguyen AV, Evans GM, Dao DV, Nguyen NT (2016b) Measuring the coefficient of friction of a small floating liquid. Marble Sci Rep 6:38346
Ooi CH, Plackowski C, Nguyen AV, Vadivelu RK, John JAS, Dao DV, Nguyen N-T (2016c) Floating mechanism of a small liquid marble. Sci Rep 6:21777
Paven M, Mayama H, Sekido T, Butt H-J, Nakamura Y, Fujii S (2016) Liquid marbles: light-driven delivery and release of materials using liquid marbles. Adv Funct Mater 26:19 /2:3372–3372
Sarvi F et al (2015) Cardiogenesis of embryonic stem cells with liquid marble micro-bioreactor. Adv Healthc Mater 4:77–86
Tian J, Fu N, Chen XD, Shen W (2013) Respirable liquid marble for the cultivation of microorganisms. Colloids Surf B 106:187–190
Ueno K, Hamasaki S, Wanless EJ, Nakamura Y, Fujii S (2014) Microcapsules fabricated from liquid marbles stabilized with latex particles Langmuir 30:3051–3059
Vadivelu RK et al (2015) Generation of three-dimensional multiple spheroid model of olfactory ensheathing cells using floating liquid marbles. Sci Rep 5:15083
Wang X, Wang X-B, Gascoyne PRC (1997) General expressions for dielectrophoretic force and electrorotational torque derived using the Maxwell stress tensor method. J Electrostat 39:277–295
Xue Y, Wang H, Zhao Y, Dai L, Feng L, Wang X, Lin T (2010) Magnetic liquid marbles: a "precise". Miniature Reactor Adv Mater 22:4814–4818
Zang D, Chen Z, Zhang Y, Lin K, Geng X, Binks BP (2013) Effect of particle hydrophobicity on the properties of liquid water marbles. Soft Matter 9:5067
Zang D, Li J, Chen Z, Zhai Z, Geng X, Binks BP (2015) Switchable Opening and closing of a liquid marble via ultrasonic levitation Langmuir 31:11502–11507
Zhang L, Cha D, Wang P (2012) Remotely controllable liquid marbles Adv Mater 24:4756–4760
Zhao Y, Fang J, Wang H, Wang X, Lin T (2010) Magnetic liquid marbles: manipulation of liquid droplets using highly hydrophobic Fe3O4. Nanoparticles Adv Mater 22:707–710
Zhao Y, Xu ZG, Parhizkar M, Fang J, Wang XG, Lin T (2012) Magnetic liquid marbles, their manipulation and application in optical probing. Microfluid Nanofluid 13:555–564
Zhu GP, Nguyen NT, Ramanujan RV, Huang XY (2011) Nonlinear deformation of a ferrofluid droplet in a uniform magnetic field Langmuir 27:14834–14841